# Single-Photon Generation from Stored Excitation in an Atomic Ensemble

C. W. Chou, S. V. Polyakov, A. Kuzmich,* and H. J. Kimble

*Norman Bridge Laboratory of Physics 12-33, California Institute of Technology, Pasadena, California 91125, USA*

(Received 21 January 2004; published 25 May 2004)

Single photons are generated from an ensemble of cold Cs atoms via the protocol of Duan *et al.* [Nature (London) **414**, 413 (2001)]. Conditioned upon an initial detection from field 1 at 852 nm, a photon in field 2 at 894 nm is produced in a controlled fashion from excitation stored within the atomic ensemble. The single-quantum character of field 2 is demonstrated by the violation of a Cauchy-Schwarz inequality, namely $w(1_2, 1_2|1_1) = 0.24 \pm 0.05 \not\geq 1$, where $w(1_2, 1_2|1_1)$ describes the detection of two events $(1_2, 1_2)$ conditioned upon an initial detection $1_1$, with $w \to 0$ for single photons.

DOI: 10.1103/PhysRevLett.92.213601 PACS numbers: 42.50.Dv, 03.67.–a, 42.65.–k

A critical capability for quantum computation and communication is the controlled generation of single-photon pulses into well-defined spatial and temporal modes of the electromagnetic field. Indeed, early work on the realization of quantum computation utilized single-photon pulses as quantum bits (*flying qubits*), with nonlinear interactions mediated by an appropriate medium [1,2]. More recently, a scheme for quantum computation by linear optics and photoelectric detection has been developed that again relies upon single-photon pulses as qubits [3]. Protocols for the implementation of quantum cryptography [4] and of distributed quantum networks also rely on this capability [5,6], as do some models for scalable quantum computation [7].

Efforts to generate single-photon wave packets can be broadly divided into techniques that provide photons "on demand" (e.g., quantum dots [8–10] or single atoms [11] coupled to microcavities) and those that produce photons as a result of conditional measurement on a correlated quantum system. For conditional generation, the detection of one photon from a correlated pair results in a one-photon state for the second photon, as was first achieved using "twin" photons from atomic cascades [12,13] and parametric down-conversion [14], with many modern extensions [15–18]. A remarkable protocol for scalable quantum networks [6] suggests a new avenue for producing single photons via conditional measurement of the light from optically thick atomic samples [19,20].

Inspired by the protocol of Ref. [6], in this Letter we report a significant advance in the creation of single photons for diverse applications in quantum information science, namely, the generation and storage of single quanta in an atomic ensemble. As illustrated in Fig. 1, an initial *write* pulse of (classical) light creates a state of collective excitation in an ensemble of cold atoms as determined by photoelectric detection for the generated field 1. Although this first step is probabilistic, its success heralds the preparation of one excitation stored within the atomic medium. After a programmable delay $\delta t$, a *read* pulse converts the state of atomic excitation into a field excitation, generating one photon in a well-defined spatial and temporal mode 2. The quantum character of the (1, 2) fields is demonstrated by the observed violation of a Cauchy-Schwarz inequality [21–23]. The improvement of nonclassical correlation for photon pairs for the (1, 2) fields reported here enables the conditional generation of single photons, now with the photon stored as an excitation in the atomic ensemble before retrieval [16].

Figure 1 provides an overview of our experiment for producing correlated photons from an optically thick sample of four-level atoms in a magneto-optical trap (MOT) [21,24]. The ground states $\{|a\rangle; |b\rangle\}$ correspond to the $6S_{1/2}, F = \{4; 3\}$ levels in atomic Cs, while the excited states $\{|e\rangle; |e'\rangle\}$ denote the $\{6P_{3/2}, F = 4; 6P_{1/2}, F = 4\}$ levels of the $D_2$, $D_1$ lines at $\{852; 894\}$ nm, respectively. We start the protocol for single-photon generation by shutting off all light responsible for trapping and cooling for 1 $\mu$s, with the trapping light turned off approximately 300 ns before the repumping light in order to empty the $F = 3$ hyperfine level in the Cs $6S_{1/2}$ ground state, thus preparing the atoms in $|a\rangle$. During the "dark"

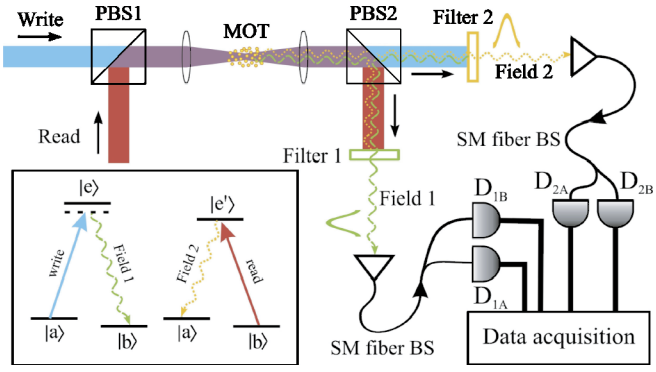


FIG. 1 (color online). Schematic of experiment for conditional generation of single photons. *Write* and *read* pulses sequentially propagate into a cloud of cold Cs atoms (MOT), generating the correlated output fields (1, 2). A detection event for field 1 at $D_{1A,1B}$ leads to an approximate one-photon state for field 2, as confirmed with detectors $D_{2A,2B}$. (P)BS: (polarization) beam splitter; SM: single mode. The inset illustrates the relevant atomic level scheme.

  

period, the $j$th trial is initiated at time $t_j^{(1)}$ when a rectangular pulse from the write laser beam, 150 ns in duration (FWHM) and tuned 10 MHz below the $|a\rangle \rightarrow |e\rangle$ transition, induces spontaneous Raman scattering to level $|b\rangle$ via $|a\rangle \rightarrow |e\rangle \rightarrow |b\rangle$. The write pulse is sufficiently weak so that the probability to scatter one Raman photon into a forward propagating wave packet $\psi^{(1)}(\vec{r}, t_j^{(1)})$ is much less than unity for each pulse. The detection of one photon from field 1 results in a "spin" excitation to level $|b\rangle$, with this excitation distributed in a symmetrized, coherent manner throughout the sample of $N$ atoms illuminated by the write beam.

Given this initial detection, the stored atomic excitation can be converted into one photon at a user controlled time $t_j^{(2)} = t_j^{(1)} + \delta t$. To implement this conversion, a rectangular pulse from the read beam, 120 ns in duration (FWHM) and resonant with the $|b\rangle \rightarrow |e'\rangle$ transition, illuminates the atomic sample. This pulse affects the transfer $|b\rangle \rightarrow |e'\rangle \rightarrow |a\rangle$ with the accompanying emission of field 2 on the $|e'\rangle \rightarrow |a\rangle$ transition described by the wave packet $\psi^{(2)}(\vec{r}, t_j^{(2)})$. The spatial and temporal structure of $\psi^{(1,2)}(\vec{r}, t)$ are discussed in detail in Ref. [25]. The trapping and repumping light for the MOT are then turned back on to prepare the atoms for the next trial $j + 1$. The whole process is repeated at 250 kHz.

The forward-scattered Raman light from the write, read pulses is directed to two sets of single-photon detectors ($D_{1A,1B}$ for field 1 and $D_{2A,2B}$ for field 2), with overall efficiencies $(\alpha_1, \alpha_2) = (0.10, 0.094)$ [26]. Light from the (write, read) pulses is strongly attenuated (by $\simeq 10^6$) by the filters shown in Fig. 1, while the associated fields (1, 2) are transmitted with high efficiency ( $\simeq 80\%$) [21]. Detection events from $D_{1A,1B}$ within the intervals $[t_j^{(1)}, t_j^{(1)} + T]$ and from $D_{2A,2B}$ within $[t_j^{(2)}, t_j^{(2)} + T]$ are time stamped (with a resolution of 2 ns) and stored for later analysis. $T = 200$ ns for all of our measurements.

For a particular set of operating conditions, we determine the single $p_l$ and joint $p_{l,m}$ event probabilities from the record of detection events at $D_{1A,1B}, D_{2A,2B}$, where $(l, m) = 1$ or 2. The total singles probability $p_l$ for events at $D_{lA}, D_{lB}$ due to field $l$ is found from the total number of detection events $n_{lA}, n_{lB}$ recorded by $D_{lA}, D_{lB}$ during the intervals $[t_j^{(l)}, t_j^{(l)} + T]$ over $M_{\text{tot}}$ repeated trials $\{j\}$, with then $p_l = (n_{lA} + n_{lB})/M_{\text{tot}}$. To determine $p_{l,l}$ for joint detections at $D_{lA}, D_{lB}$, we count the total number of coincidences $N_{lA,lB}$ recorded by $D_{lA}, D_{lB}$, with then $p_{l,l} = N_{lA,lB}/M_{\text{tot}}$. Joint detections between the (1, 2) fields are described by $p_{1,2}$, which is determined by summing coincidence events between the four pairs of detectors for the (1, 2) fields (e.g., between pairs $D_{1A}, D_{2A}$).

From $(p_l, p_{l,m})$ we derive estimates of the normalized intensity correlation functions $\tilde{g}_{l,m}$, where $\tilde{g}_{l,m} = 1$ for coherent states. For example, the autocorrelation function $\tilde{g}_{1,1} = p_{1,1}/(p_{1A}p_{1B})$ for field 1, and similarly for the functions $\tilde{g}_{2,2}, \tilde{g}_{1,2}$ for the autocorrelation of field 2 and the cross correlation between fields (1, 2). The first column in Fig. 2 displays $\tilde{g}_{1,1}$, $\tilde{g}_{2,2}$, and $\tilde{g}_{1,2}$ as functions of $p_1$, $p_2$, and $\sqrt{p_1 p_2}$ [27]. A virtue of $\tilde{g}_{l,m}$ is its independence from the propagation and detection efficiencies. In the ideal case, the state for the fields (1, 2) is [6,23,25]

$$|\Phi_{12}\rangle = |0_1 0_2\rangle + \sqrt{\chi}|1_1 1_2\rangle + \chi|2_1 2_2\rangle + O(\chi^{3/2}), \quad (1)$$

where $\sqrt{\chi}$ is the excitation amplitude for field 1 in each trial of the experiment. For $\chi \ll 1$, $\tilde{g}_{1,1} = \tilde{g}_{2,2} = 2$ and $\tilde{g}_{1,2} = 1 + 1/\chi$. By contrast, for reasons that we address shortly, our measurements in Fig. 2 give $\tilde{g}_{1,1} \simeq 1.7$ and $\tilde{g}_{2,2} \simeq 1.3$, with $\tilde{g}_{1,2}$ exhibiting a sharp rise with decreasing $\sqrt{p_1 p_2}$, but with considerable scatter.

To provide a characterization of fields (1, 2) that is independent of the efficiency of our detection setup, we convert the photodetection probabilities $(p_l, p_{l,m})$ to the quantities $(q_l, q_{l,m})$ for the field mode collected by our imaging system at the output of the MOT. Explicitly, for single events for fields (1, 2), we define $q_l \equiv p_l/\alpha_l$, while for joint events, $q_{l,m} \equiv p_{l,m}/\alpha_l\alpha_m$, where $\alpha_{l,m}$ gives the overall efficiencies for fields (1, 2) [26]. The second column in Fig. 2 displays the measured dependence of $q_{l,m}$ for joint events on $q_1$, $q_2$, $\sqrt{q_1 q_2}$ for single events over a range of operating conditions. As expected from Eq. (1), $q_{1,1}$, $q_{2,2}$ exhibit an approximately quadratic dependence on $q_1$, $q_2$, while $q_{1,2}$ is roughly linear for $\sqrt{q_1 q_2} \ll 1$. Beyond the statistical uncertainties shown in Fig. 2, there are clearly much larger systematic deviations. The detailed mechanisms responsible for these deviations are

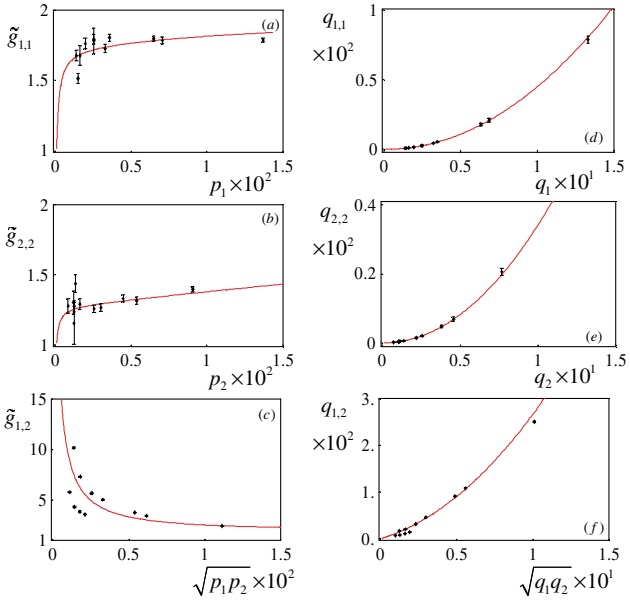


FIG. 2 (color online). Left column: (a)–(c) Normalized intensity correlation functions $\tilde{g}_{1,1}$, $\tilde{g}_{2,2}$, $\tilde{g}_{1,2}$ versus observed detection probabilities $p_1$, $p_2$, $\sqrt{p_1 p_2}$, respectively. Right column: (d)–(f) $q_{1,1}$, $q_{2,2}$, $q_{1,2}$ for joint detection versus $q_1$, $q_2$, $\sqrt{q_1 q_2}$ for single detection, with $q_l, q_{l,m}$ referenced to the output of the MOT. Statistical uncertainties are indicated by the error bars. The full curves are from the model calculation described in the text with $(\kappa_1, \kappa_2) = (0.17, 0.90)$ and $(|v_{1b}|^2, |v_{2b}|^2) = 0.006$.

currently under investigation, and include slow drifts in optical alignment for the write, read, and (1, 2) beams.

In our experiment there are a number of imperfections that lead to deviations from the ideal case expressed by $|\Phi_{12}\rangle$ [6,23,25]. To quantify this, we developed a simple model that assumes the total fields (1, 2) at the output of the MOT consist of contributions from $|\Phi_{12}\rangle$ and background fields in coherent states $|v_{1,2}\rangle$. Operationally, $p_1$, $p_2$ are controlled by the intensity of the write beam, with only minor adjustments to the read beam. Hence, we parametrize our model by taking $\chi = |v_w|^2$, with $v_w$ as the (scaled) amplitude of the write beam. Since important sources of noise are light scattering from the write and read beams and background fluorescence from uncorrelated atoms in the sample [25], we assume that $v_{1,2} = \sqrt{\kappa_{1,2}} v_w$. We further allow for fixed incoherent backgrounds $v_{1b}, v_{2b}$ to account for processes that do not depend upon increases in write beam intensity.

With this model, we compute the quantities that appear in Figs. 2–4. The parameters $(\kappa_1, \kappa_2) = (0.17, 0.90)$ and $(|v_{1b}|^2, |v_{2b}|^2) = 0.006$ are obtained directly by optimizing the comparison between the model results and our measurements of normalized correlation functions (e.g., $\tilde{g}_{1,1}$ vs $\tilde{g}_{1,2}$) without requiring absolute efficiencies. $\kappa_1 = 0.17$ implies that the photon number for "good" events associated with $|\Phi_{12}\rangle$ exceeds that for "bad" (background) events from $|v_1\rangle$ by roughly sixfold for detection at $D_{1A}$, $D_{1B}$. For the curves in Fig. 2, we must also obtain the efficiencies $\beta_l$, $\eta_l$ that convert expectation values for normally ordered photon number operators $\hat{n}_l$ for fields $l = (1, 2)$ in the model into the various $(p_l, p_{l,m})$ and $(q_l, q_{l,m})$ (e.g., $p_l = \beta_l \langle \hat{n}_l \rangle$, $q_l = \eta_l \langle \hat{n}_l \rangle$, $q_{1,2} = \eta_1 \eta_2 \langle : \hat{n}_1 \hat{n}_2 : \rangle$). Ideally $\beta_l = \alpha_l$ and $\eta_l = 1$; we find instead $(\beta_l, \eta_l) = (0.013, 0.15)$, where we take $\beta_1 = \beta_2$ and $\eta_1 = \eta_2$ for simplicity. Among various candidates under investigation, values $\beta_l < \alpha_l$, $\eta_l < 1$ can arise from inherent mode mismatching for capturing collective emission from the atomic ensemble [25].

Following the pioneering work of Clauser [12], we utilize the results from Fig. 2 to address directly the question of the nonclassical character of the (1, 2) fields independent of absolute efficiencies. The correlation functions $\tilde{g}_{l,m}$ for fields for which the Glauber-Sudarshan phase-space function $\varphi$ is well behaved (i.e., *classical* fields) are constrained by the inequality $R \equiv [\tilde{g}_{1,2}]^2 / \tilde{g}_{1,1} \tilde{g}_{2,2} \leq 1$ [12,23]. In Fig. 3 we plot the experimentally derived values for $R$ versus the degree of cross correlation $\tilde{g}_{1,2}$ [27]. As compared to previous measurements for which $R = 1.84 \pm 0.06$ [21] and $R = 1.34 \pm 0.05$ [22], we have achieved $R = (53 \pm 2) \gg 1$. In Figs. 2–4, all points are taken with $\delta t = 200$ ns, except the points at $\tilde{g}_{1,2} \simeq 10$, which have $\delta t = 50$ ns.

This large degree of quantum correlation between the (1, 2) fields suggests the possibility of producing a single-photon in field 2 by conditional detection of field 1. To investigate this, we consider the correlation function $w(1_2, 1_2|1_1)$ for detection with the setup shown in Fig. 1,

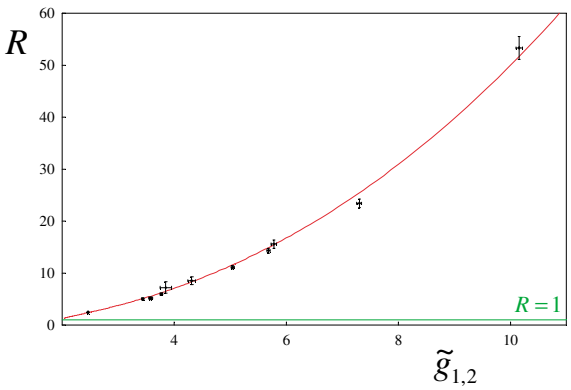


FIG. 3 (color online). Ratio $R \equiv [\tilde{g}_{1,2}]^2 / \tilde{g}_{1,1} \tilde{g}_{22}$ versus the normalized cross correlation $\tilde{g}_{1,2}$, where $R > 1$ for manifestly quantum (nonclassical) fields. The points are from our experiment with statistical uncertainties indicated by the error bars. The full curve is from the model calculation with $(\kappa_1, \kappa_2)$ and $(|v_{1b}|^2, |v_{2b}|^2)$ as in Fig. 2.

where $w(1_2, 1_2|1_1) \equiv p^{(c)}(1_2, 1_2|1_1) / [p^{(c)}(1_2|1_1)]^2$. Here, $p^{(c)}(1_2, 1_2|1_1)$ is the conditional probability for the detection of two photons $(1_2, 1_2)$ from field 2 conditioned upon the detection of an initial photon $1_1$ for field 1, and $p^{(c)}(1_2|1_1)$ is the probability for the detection of one-photon $1_2$ given a detection event $1_1$. Bayes's theorem allows the conditional probabilities to be written in terms of single and joint probabilities, so that

$$w \equiv w(1_2, 1_2|1_1) = \frac{p^{(1)}(1_1) p^{(3)}(1_1, 1_2, 1_2)}{[p^{(2)}(1_1, 1_2)]^2}. \qquad (2)$$

Classical fields must satisfy the Cauchy-Schwarz inequality $w \geq 1$; for independent coherent states, $w = 1$, while for thermal beams, $w = 2$. However, for the state $|\Phi_{12}\rangle$ of Eq. (1), $w = 4\chi \ll 1$ for small $\chi$, approaching the ideal case $w \to 0$ for a twin Fock state $|1_1 1_2\rangle$.

From the record of photodetection events at $D_{lA,lB}$, we calculate estimates of the probabilities appearing in Eq. (2), with the results of this analysis shown in Fig. 4. Part 4(a) examines the quantity $w_{i,j}$ obtained from events taken from different trials $i \neq j$ for the (1, 2) fields (i.e., detection $1_1$ in trial $i$ for field 1 followed by two detections $(1_2, 1_2)$ in trial $j$ for field 2). In this case, the (1, 2) fields should be statistically independent [23], so that $w_{i,j} = \tilde{g}_{2,2}$. Hence, we also superimpose $\tilde{g}_{2,2}$ from Fig. 2 and find reasonable correspondence within the statistical uncertainties (in particular, $w_{i,j} \gtrsim 1$), thereby validating our analysis techniques [27].

Figure 4(b) displays $w_{i,i}$ for events from the same experimental trial $i$ for the (1, 2) fields. Significantly, as the degree of cross correlation expressed by $\tilde{g}_{1,2}$ increases (i.e., decreasing $\chi$), $w_{i,i}$ drops below the classical level of unity, indicative of the sub-Poissonian character of the conditional state of field 2. With $\delta t = 200$ ns, $w_{i,i} = 0.34 \pm 0.06$ for $\tilde{g}_{1,2} = 7.3$, while with $\delta t = 50$ ns, $w_{i,i} = 0.24 \pm 0.05$ for $\tilde{g}_{1,2} = 10.2$. Beyond the comparison to our model shown in the figure, empirically we find that

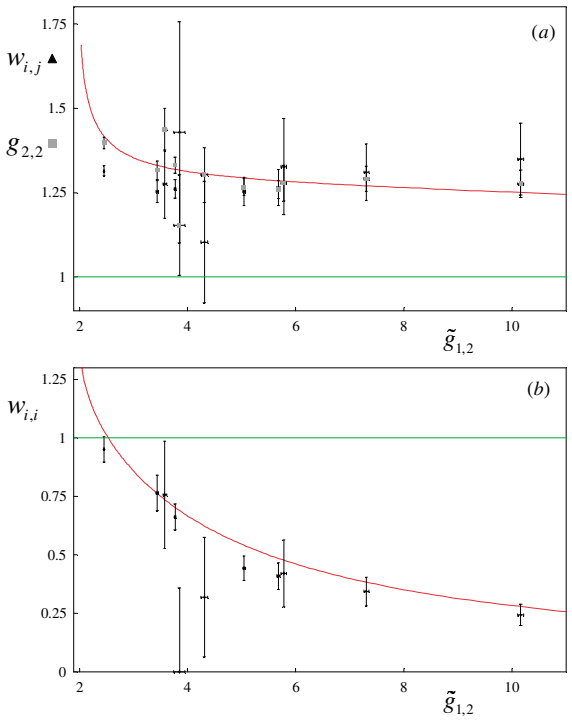


FIG. 4 (color online). Threefold correlation function $w$ for detection event $1_1$ for field 1 followed by two events $(1_2, 1_2)$ for field 2 versus the normalized cross correlation $\tilde{g}_{1,2}$. (a) $w_{i,j}$ for events $(1_1)_i$ and $(1_2, 1_2)_j$ from different trials $i \neq j$ together with points for $\tilde{g}_{2,2}$. $w_{i,j} = \tilde{g}_{2,2}$ for statistically independent trials. (b) $w_{i,i}$ for events from the same trial $i$. $w_{i,i} < 1$ for sub-Poissonian fields in support of the single-photon character of field 2. Statistical uncertainties are indicated by the error bars. The full curves are from the model calculation with $(\kappa_1, \kappa_2)$ and $(|v_{1b}|^2, |v_{2b}|^2)$ as in Figs. 2 and 3.

$w_{i,i}$ is well approximated by $\tilde{g}_{1,1}\tilde{g}_{2,2}/\tilde{g}_{1,2}$, as in the ideal case of Eq. (1). However, independent of such comparisons, we stress that the observations reported in Fig. 4 represent a sizable nonclassical effect in support of the conditional generation of single photons for field 2. No corrections for dark counts or other backgrounds have been applied to the data in Fig. 4 (nor, indeed, to Figs. 2 and 3).

In conclusion, our experiment represents an important step in the creation of an efficient source of single photons stored within an atomic ensemble, and thereby towards enabling diverse protocols in quantum information science [3,4,6,7]. Our model supports the hypothesis that the inherent limiting behavior of $w_{i,i}$ below unity is set by the efficiency $\eta_l$, which leads to prohibitively long times for data acquisition for $\chi \lesssim 0.04$, corresponding to the smallest value of $w_{i,i}$ in Fig. 4. We are pursuing improvements to push $\eta_l \simeq 0.15 \rightarrow 1$. Dephasing due to Larmor precession in the quadrupole field of the MOT limits $\delta t \lesssim 300$ ns, which can be extended to several seconds in optical dipole or magnetic traps [24].

We gratefully acknowledge the contributions of A. Boca, D. Boozer, W. Bowen, and L.-M. Duan. This work is supported by ARDA, by the Caltech MURI Center for Quantum Networks, and by the NSF.

*Present address: School of Physics, Georgia Institute of Technology, Atlanta, Georgia 30332, USA.

[1] I. L. Chuang and Y. Yamamoto, Phys. Rev. A **52**, 3489 (1995).
[2] Q. A. Turchette *et al.*, Phys. Rev. Lett. **75**, 4710 (1995).
[3] E. Knill, R. Laflamme, and G. Milburn, Nature (London) **409**, 46 (2001).
[4] N. Lutkenhaus, Phys. Rev. A **61**, 052304 (2000).
[5] H.-J. Briegel and S. J. van Enk, in *The Physics of Quantum Information*, edited by D. Bouwmeester, A. Ekert, and A. Zeilinger (Springer-Verlag, Berlin, 2000), Vols. 6.2 and 8.6.
[6] L.-M. Duan *et al.*, Nature (London) **414**, 413 (2001).
[7] L.-M. Duan and H. J. Kimble, Phys. Rev. Lett. **92**, 127902 (2004).
[8] P. Michler *et al.*, Science **290**, 2282 (2000).
[9] E. Moreau *et al.*, Appl. Phys. Lett. **79**, 2865 (2001).
[10] M. Pelton *et al.*, Phys. Rev. Lett. **89**, 233602 (2002).
[11] J. McKeever *et al.*, Science **303**, 1992 (2004).
[12] J. F. Clauser, Phys. Rev. D **9**, 853 (1974).
[13] P. Grangier, G. Roger, and A. Aspect, Europhys. Lett. **1**, 173 (1986).
[14] C. K. Hong and L. Mandel, Phys. Rev. Lett. **56**, 58 (1986).
[15] A. I. Lvovsky *et al.*, Phys. Rev. Lett. **87**, 050402 (2001).
[16] T. B. Pittman, B. C. Jacobs, and J. D. Franson, Phys. Rev. A **66**, 042303 (2002).
[17] J. B. Altepeter *et al.*, Phys. Rev. Lett. **90**, 193601 (2003).
[18] A. B. U'Ren *et al.*, quant-ph/0312118.
[19] B. Julsgaard *et al.*, Q. Inf. Computation **3**, 518 (2003).
[20] M. Lukin, Rev. Mod. Phys. **75**, 457 (2003).
[21] A. Kuzmich *et al.*, Nature (London) **423**, 731 (2003).
[22] Wei Jiang *et al.*, quant-ph/0309175.
[23] Supplementary information accompanying Ref. [21] at http://www.nature.com/nature/journal/v423/n6941/suppinfo/nature01714.html.
[24] *Laser Cooling and Trapping*, edited by H. J. Metcalf and P. van der Straten (Springer-Verlag, Berlin, 1999).
[25] L.-M. Duan, J. I. Cirac, and P. Zoller, Phys. Rev. A **66**, 023818 (2002).
[26] The overall efficiencies $\alpha_{1,2} = \xi_{1,2}T_{1,2}\varsigma_{1,2}$, where $\xi_{1,2} = (0.41 \pm 0.04, 0.47 \pm 0.04)$ for light with the spatial shape of the *write, read* beams propagating from the MOT to the input beam splitters for detectors $(D_{1A,1B}, D_{2A,2B})$, which have quantum efficiencies $\varsigma_{1,2} \simeq (0.50, 0.40)$ (i.e., photon *in* to electronic pulse *out*). The efficiencies $T_{1,2} = 0.50$ for PBS2 in Fig. 1 account for the presumed unpolarized character of the (1, 2) fields in our experiment.
[27] To check various experimental procedures, we have employed white light to make the same measurements of $\tilde{g}_{1,1}$, $\tilde{g}_{2,2}$, $\tilde{g}_{1,2}$, and $w_{i,i}$ as were made in Figs. 2–4, and find that $\tilde{g}_{1,1} = 1.02 \pm 0.01$, $\tilde{g}_{2,2} = 1.01 \pm 0.01$, $\tilde{g}_{1,2} = 1.02 \pm 0.01$, $w_{i,i} = 0.99 \pm 0.2$, $w_{i,j} = 0.97 \pm 0.02$, where in all cases, these correlation functions should equal unity.